DOI: 10.13009/EUCASS2019-891

8TH EUROPEAN CONFERENCE FOR AERONAUTICS AND AEROSPACE SCIENCES (EUCASS)

DOI: ADD DOINUMBER HERE

Direct numerical simulations of swirled jet sprays

P. P. Ciottoli[⋆], *R. Malpica Galassi*[⋆†], *P.Gualtieri*[⋆], *F. Battista*[§], *F. Dalla Barba*[¶], *M. Valorani*[⋆] *and F. Picano*[¶]
[⋆] *Dept. of Mechanical and Aerospace Engineering, Sapienza University of Rome, Italy*
[§] *ENEA C.R. Casaccia, Rome, Italy*
[¶] *Department of Industrial Engineering, University of Padova, Italy*
riccardo.malpicagalassi@uniroma1.it
[†]Corresponding author

Abstract

The effects of a swirled inflow on turbulent jet laden with acetone droplets injected in fresh air are investigated by means of direct numerical simulation. The numerical framework is based on a hybrid Eulerian-Lagrangian approach, and the point droplet approximation. Both a phenomenological and a statistical analysis of both phases are presented. The sensitivity of the evaporation processes to swirl are discussed.

1. Introduction

Turbulent sprays are complex multiphase flows playing an important role in several technological devices as well as in natural processes. This class of phenomena involves unsteady and multiscale processes such as turbulent flow motions and dispersed phase transition processes. The main challenges in tackling the problem arise from the mutual interaction of two distinguished phases, consisting in mass, momentum, and energy exchange. Although a satisfactory comprehension of the turbulent spray dynamics has not yet been achieved, research progress in this field is a key enabling technology for several industrial applications, towards efficiency increase, emissions reduction and control. As an example, in internal combustion engines, as well as aeronautical engines, liquid fuel is directly injected into the combustion chamber, where the vaporization of fuel droplets occurs together with chemical reactions within the turbulent gaseous environment. The formation of pollutants in turbulent flows is related to multiscale phenomena that involve fluctuations of temperature and reactants concentrations.

A physical description of the liquid and gaseous phases interaction bringing from bulk liquid to sprays can be found in the work of of Lefebvre and McDonell,[11] while a phenomenological description of the spray dynamics is reported in the review of Jenny et al.[9] The atomization dynamics is controlled by the competition between the liquid surface tension and the gaseous stresses acting on the two-phase interface. Firstly, the liquid jet, interacting with the gaseous environment, experiences a primary atomization. In this phase, interface instabilities such as Kelvin-Helmholtz and Rayleigh-Taylor fragmentize the jet into large drops and liquid ligaments [6]. The dispersed liquid phase is now referred to as in dense spray regime. If the aerodynamic forces acting on the liquid, and arising from the relative interphase velocities, cause instabilities, these result in a further disintegration named secondary breakup. The dispersed liquid phase is now referred to as in dilute spray regime, characterized by smaller drops, the atomization process terminates when the surface tension prevails on aerodynamic stresses preventing further fragmentation. Although in the dilute regime droplet mutual interactions, such as collisions and coalescence, are negligible, the effect of droplets on the gaseous phase are not, as demonstrated via direct numerical simulation by Krebs et al.[10] and Gualtieri et al.[8] among the others.

In contrast with the dense regime, in which the surface-to-volume ratio is low enough to make vaporization rate negligible, in the dilute regime most of the liquid evaporates and vaporization becomes significant. Moreover, smaller droplets are characterized by the dominance of the surface tension on the aerodynamic stresses this resulting in a spherical shape. Finally, in this regime, droplet size is usually comparable or smaller than the smallest scales of the turbulent flow, so that the point droplet approximation can be successfully employed as demonstrated by Elghobashi.[5] Nonetheless, droplets exert a non-negligible effect on the gaseous flow in terms of mass, momentum, and energy balance.[5]

For the aforementioned reasons, a hybrid Eulerian-Lagrangian description results to be a good candidate for the mathematical description of droplet-laden flows in dilute conditions. The Eulerian-Lagrangian description[2,9] ensures the two-way coupling between the two phases by resolving the classical Navier-Stokes equations for the gaseous carrier flow, with additional sink-source terms to represent the mass, momentum, and energy exchanges between the Eulerian

DOI: 10.13009/EUCASS2019-891

carrier phase and Lagrangian point droplets. Each droplet is simultaneously evolved in a Lagrangian point fashion, while the aerodynamic forces governing their motion are computed as a function of the continuous carrier flow.

2. Motivations

In the direct numerical simulation framework, the hybrid Eulerian-Lagrangian approach can be achieved by means of well established sub-models meant to take into account the mutual effects of the two phases. Nonetheless, when dealing with large eddy simulation (LES) or Reynolds averaged Navier Stokes (RANS) approaches, in which only the larger scales are resolved, the interaction of the small scale turbulent motion with the dispersed drops requires a proper modeling. In this context, a-priori direct numerical simulation (DNS) studies can help isolating the main features of the small scale fluid drops interaction, and can guide the formulation of proper closure sub-models for both RANS and LES Eulerian-Lagrangian formulations. A fundamental study of the effects of the entrainment in an evaporating turbulent jet spray in combination with an analysis of the preferential segregation effect was carried out by Dalla Barba and Picano[2] considering DNS data of an evaporating turbulent spray, using a two-way coupling approach between the two phases and accounting for the entrainment effect. Two different mechanisms were found to drive preferential segregation: the first due to the inertial clustering; the second related to the dynamics of the jet entrainment. This latter mechanism was found to be crucial in the outer part of the jet core, where the evaporation peaks, and strongly impacts the vaporization process, which was found to be characterized by an extreme widening of the droplet size spectrum. This work aims at extending the study of Dalla Barba and Picano[2] by investigating the sensitivity to swirl of a jet spray vaporization processes.

3. Test case description

All the presented DNS computations reproduce liquid acetone droplets dispersed within a turbulent air-acetone vapor jet.

With the only exception of a lower Reynolds number, the flow conditions at the inlet section are comparable to those adopted in the well-controlled experiments on dilute coaxial sprays published by the group of Masri and coworkers[4] and Villermaux et al.,[16] which used acetone droplets dispersed in air at the temperature of $275.15K$ in both non-reactive and reactive conditions. The gas-vapor mixture is injected into an open environment through an orifice of radius R = $5 \cdot 10^{-3}$ m at a bulk axial velocity $U_{z,0} = 8.1m/s$. The spray distribution in the inflow section consists of a random distribution of liquid acetone monodisperse droplets with initial radius $r_{d,0} = 6\mu m$. The ambient pressure is set to $p_0 = 101300Pa$, the injection temperature is fixed to $T_0 = 275.15K$ for both carrier and disperse phases. The injection flow rate of the gaseous phase is kept constant fixing a bulk Reynolds number $Re = 2U_0R/\nu = 6000$, being $\nu = 1.35 \cdot 10 - 5m^2/s$ the kinematic viscosity. A nearly saturated condition is prescribed for the air-acetone vapor mixture at the inflow section, with saturation $S = Y_v/Y_{v,s} = 0.99$, where Y_v is the actual vapor mass fraction and $Y_{v,s}(p_0, T_0)$ is the vapor mass fraction saturation level evaluated at the inflow temperature and pressure. The acetone mass flow rate has a mass flow rate ratio $\Psi = \dot{m}_{act}/\dot{m}_{air} = 0.28$, $\dot{m}_{act} = \dot{m}_{act,l} + \dot{m}_{act,v}$ being the sum of liquid, $\dot{m}_{act,l}$, and gaseous, $\dot{m}_{act,l}$, acetone mass flow rates. This configuration corresponds to a bulk volume fraction of the liquid phase $\Phi = 8 \cdot 10^{-5}$.

p_0 $[Pa]$	101300	W_g $[kg/mol]$	$2.90 \cdot 10^{-2}$
T_0 $[K]$	275.15	W_l $[kg/mol]$	$5.81 \cdot 10^{-2}$
U_0 $[m/s]$	8.10	k_g $[W/mK]$	$2.43 \cdot 10^{-2}$
μ $[kg/ms]$	$1.75 \cdot 10^{-5}$	k_l [W/mK]	$1.83 \cdot 10^{-1}$
$c_{p,g}$ $[J/(kgK)]$	1038	D $[m^2/s]$	$1.10 \cdot 10^{-5}$
$c_{p,v}$ $[J/(kgK)]$	1300	ρ_l $[kg/m^3]$	800
c_l $[J/(kgK)]$	2150	H_v $[J/kg]$	530000
R $[m]$	$5 \cdot 10^{-3}$	Ψ	0.28
Φ	$8 \cdot 10^{-5}$	ν $[m^2/s]$	$1.35 \cdot 10^{-5}$
$r_{d,0}$ $[m]$	$6 \cdot 10^{-6}$	$Re = U_0R/\nu$	3000

Table 1: Thermodynamic and physical properties of acetone and dry air

The baseline configuration[2] is characterized by a purely axial inflow velocity, the thermodynamic and physical properties of the vapor, gas, and liquid phases are summarized in Table 1. Two additional configurations are investi-

DOI: 10.13009/EUCASS2019-891

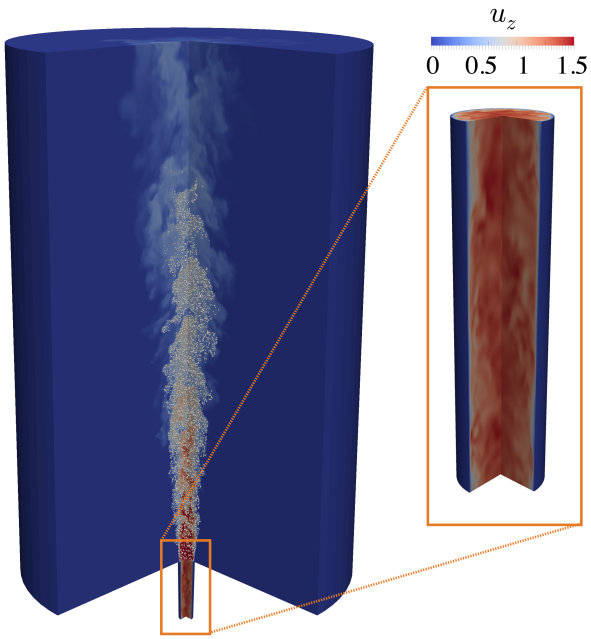

Figure 1: A sketch of the 3D cylindrical domain and the turbulent periodic pipe. A representative ensemble of the whole droplet population is plotted with white points. On the left, the colors contour the vapor mass fraction field within the jet. On the right colors contour the axial instantaneous velocity of the turbulent pipe.

gated. These two additional test cases are identical to the baseline configuration, with the only exception of the swirl number, defined as $S_w = U_t/U_{z,0}$, where U_t is the tangential velocity at the jet inflow. As reported in Table 2, the three simulations have swirl number of 0, 0.4 and 0.95 and are referred to as zero, medium, and high swirl, respectively.

1 - Zero Swirl (NS)	$Sw = 0$
2 - Medium Swirl (MS)	$Sw = 0.4$
3 - High Swirl (HS)	$Sw = 0.95$

Table 2: Swirl number values

4. Theoretical and numerical formulation

As previously mentioned, the results presented in this work are obtained by means of a DNS solution of the evaporating spray in a hybrid Eulerian-Lagrangian framework. The details of the computational framework, including the mesh resolution are detailed in the work of Dalla Barba and Picano,[2] and are here recalled for the sake of self consistency of the document.

The Eulerian gaseous phase is numerically described by means of low-Mach number asymptotic formulation of the Navier-Stokes equations in an open environment, allowing the description of density variations discarding acoustics effects.[12] The transport equations for density, vapor mass fraction Y_v, momentum, and temperature are discretized in space via finite volume approach. Consistently with previous studies in this field,[3,13,14] the effects of the dispersed phase on the gaseous carrier phase is accounted for by three sink-source coupling terms in the right-hand side of the mass, momentum, and energy equations. The aforementioned Eulerian equations are discretized by means of a second-order central finite differences scheme, on the staggered grid for space discretization,[6] and integrated in time along with an ideal-gas equation of state by means of a low-storage, third-order, Runge-Kutta scheme. For all simulations, the inflow velocity conditions are obtained assigning a fully turbulent velocity at the jet inflow section by means of a Dirichlet condition. The prescribed inflow condition is a cross-sectional slice of a fully developed DNS of a pipe flow. The flow is injected through a center orifice while the remaining part of the domain base is impermeable and

DOI: 10.13009/EUCASS2019-891

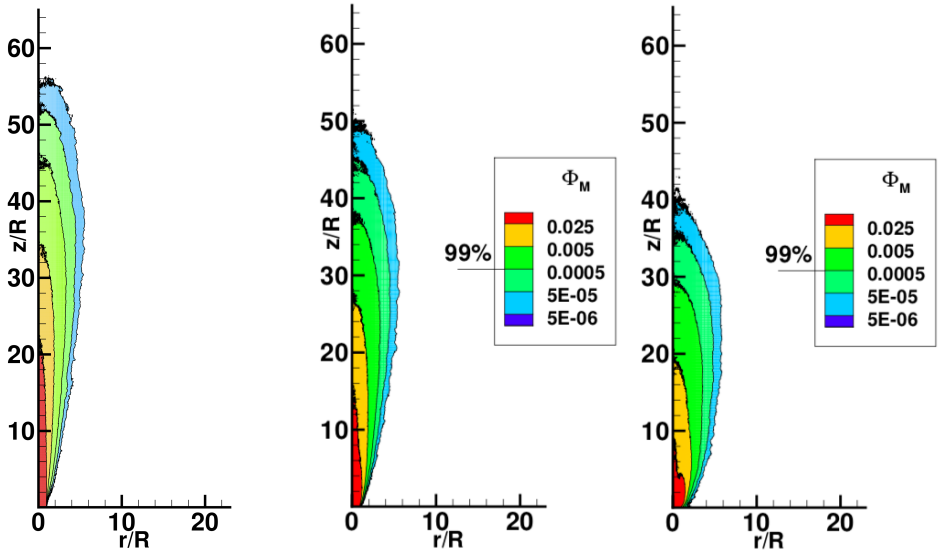

(a) (b) (c)

Figure 2: Mean liquid mass fraction,$\Phi = m_l/m_g$,where m_l and m_g are the mean mass of liquid acetone and air inside each mesh cell, respectively. From left to right: zero, medium, and hight swirl cases.

adiabatic. In the medium and high swirl test cases, the swirled profile is obtained by imposing U_t at the pipe wall, i.e. simulating a rotating pipe. A sketch of the cylindrical domain and of the turbulent periodic pipe is displayed in Fig.1. The computational domain consists of a cylinder extending for $2\pi \times 22R \times 70R$in the azimuthal, θ, radial, r, and axial, z, directions. The domain has been discretized by $N_\theta \times N_r \times N_z = 128 \times 225 \times 640$ points using a staggered mesh continuously stretched in the radial and axial direction. The mesh has been stretched to be of the order of the Kolmogorov length scale $\eta = (\nu^3/\epsilon)^{1/4}$, where ϵ is the turbulent energy dissipation, in the downstream evolution of the spray. At the jet inlet section, the maximum of the typical mesh size on the Kolmogorov length, $\Delta/\eta = [(r\Delta_\theta)rz]^{1/3}/\eta$, is about 2.4 and is kept around this value during the downstream jet evolution. The flow is injected at the center of one base of the cylindrical domain and streams out towards the other base. A convective condition is adopted at the outlet, and an adiabatic traction-free condition is prescribed at the side boundary. This side boundary condition makes the entrainment of external fluid possible, which is dry air in the present case. The turbulent periodic pipe employed as inflow boundary condition extends for $2\pi \times 1R \times 8R$ in the azimuthal, θ, radial, r, and axial, z, directions. The domain is discretized with an equispaced staggered mesh containing $N_\theta \times N_r \times N_z = 128 \times 80 \times 128$ nodes in order to match the corresponding jet computational grid at the pipe discharge.

The droplets are treated as rigid evaporating spheres, and the liquid phase properties, such as temperature, are assumed to be uniform inside each droplet. Consistently with the dilute spray conditions, droplet mutual interactions, such as collisions and coalescence, are neglected.[2] The effect of Reynolds number on the drag of droplets is taken into account by means of the Schiller-Naumann correlation.[14] The mass exchange due to droplet evaporation is modeled according to the Spalding[15] and Godsave[7] theory, assuming that the vapor mass fraction at droplet surface is the saturated vapor-gas mixture at the droplet temperature, and computing the latter by means of the Clausius-Clapeyron relation. The droplet temperature and mass variation due to mass diffusivity, and the thermal conductivity are estimated via Schmidt and Prandtl numbers, while the Nusselt and the Sherwood numbers are estimated as a function of the droplet Reynolds number according to the Frössling correlation, and further corrected to account for the Stefan flow.[1] The droplet mass, momentum, and temperature laws are evolved by means of a Lagrangian approach. The temporal integration uses the same Runge-Kutta scheme adopted by the Eulerian algorithm. Second-order accurate polynomial interpolations are used to calculate the Eulerian quantities at the droplet positions.

DOI: 10.13009/EUCASS2019-891

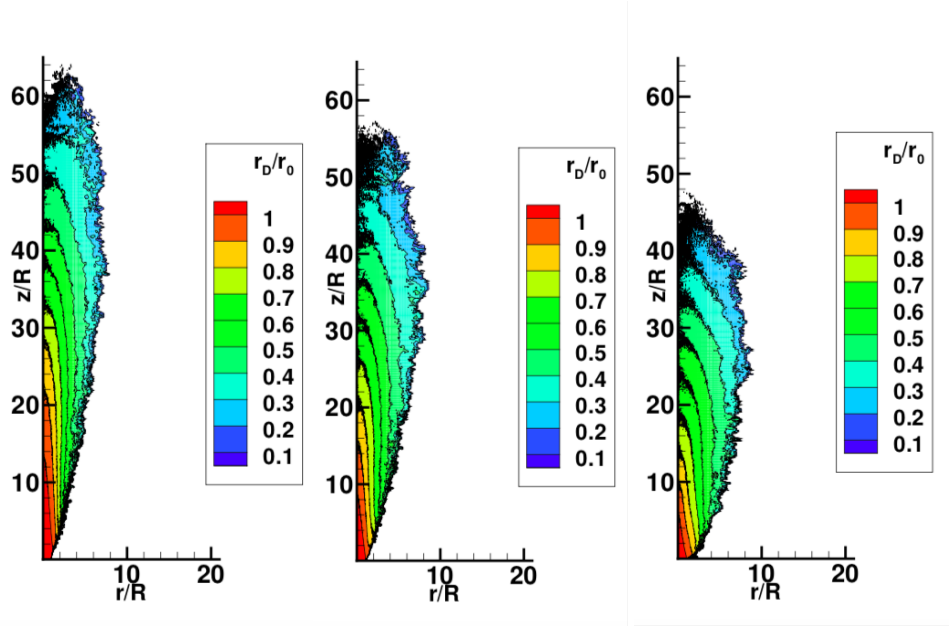

(a) (b) (c)

Figure 3: Sensitivity to swirl number of the mean droplet radius rescaled by the droplet initial radius $r_{d,0} = 6\mu m$. From left to right: zero, medium, and hight swirl cases.

5. Preliminary Results

At the moment of writing this document, although the numerical campaign is complete, the data analysis is in progress. A selection of preliminary results are provided in the following. Figure 2 shows the contour mean liquid volume fraction,Φ. The overall vaporization length, defined as the axial distance from the inflow section where the 99% of the injected liquid mass has transitioned to the vapor phase, appears to move upstream for increasing swirl number. The mean droplet radius distributions, rescaled by the droplet initial radius $r_{d,0} = 6\mu m$, are reported in Fig. 3, and suggest that, as an effect of the swirl, large drops are convected radially in proximity of the inflow, while a faster droplet radius diminution moving along the axis is observed. Consistently with the findings of previous studies,[2] the turbulent jet spray can be described as a turbulent core decaying along the axial direction, and being surrounded and entrained by dry air. In the region where, due to the entrainment, dry air meets the acetone spray, the vapour concentration diminishes, enhancing vaporization, and reducing the droplets radius. Since the effect of the dry air entrainment plays a crucial role on the overall vaporization process, the inner jet core shows higher saturation levels, being prevented from reaching the outer region. This explains why evaporation occurs mostly in the mixing layer. The swirled inflow velocity acts on the spatial location of the mixing layer, increasing the jet spread angle. This line of reasoning is confirmed by the mean droplet vaporization rate distribution, displayed in Fig.4 for the three inflow conditions, and showing that vaporization occurs in the shear layer, attaining maximum values close to the inflow orifice. Moreover, the spread angle of the evaporation region increases with the swirl intensity. In all the test cases the peak value is found in the shear layer, immediately downstream the inflow section, where large droplets enter in direct contact with the dry environmental air. This region is less elongated and more stretched in the radial direction for larger swirl numbers. Although for all test cases, for a given axial distance, the droplets radius diminishes moving away from the jet axis, the spray core extension in the axial direction diminishes with the swirl intensity. This means that the spray core, where the vaporization process is slowed by the high vapor concentration, is reduced by the swirl.

A clear picture of the sensitivity to swirl number of the droplets dimension is provided by the probability density function (PDF) of the droplet radius at different axial distances from the origin, as reported in Fig. 5. Since the inflow condition is a monodisperse suspension, in all test cases the PDF at inflow section is a Dirac function centered at $r_d/r_{d,0}$=1. Nonetheless, consistently with experimental observations in turbulent sprays,[4] even in the case of zero swirl, shown in Fig. 5-a, it is observed a radius distribution spanning around one decade after 10 jet radii from the inlet. This intense spread in the droplet radius statistical distribution is enhanced for the medium- and high-swirl test cases, shown in Figs. 5-b and 5-c respectively. As an example, the PDF of droplet distribution at x/r=10 of the high-swirl test cases,

DOI: 10.13009/EUCASS2019-891

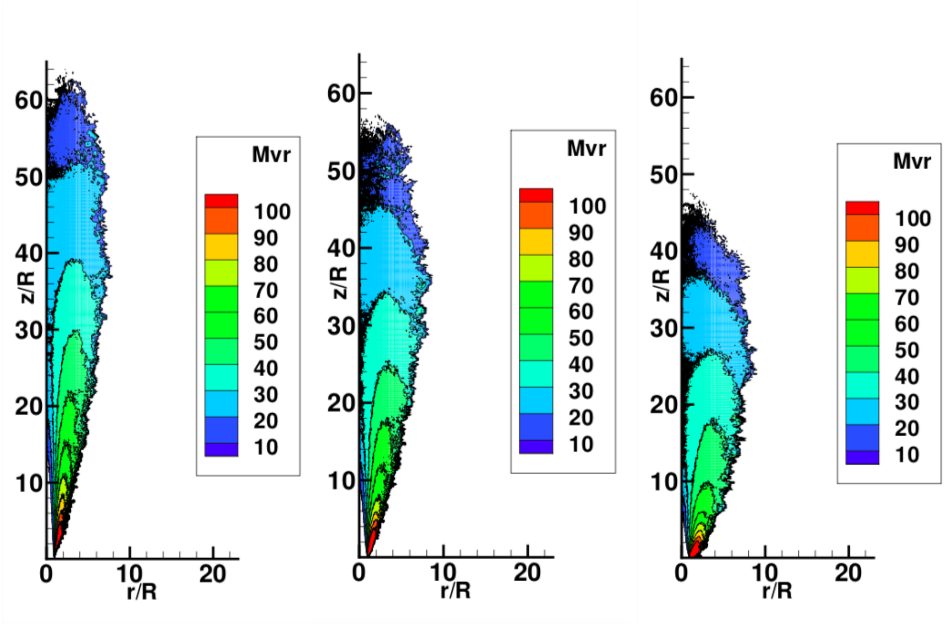

(a) (b) (c)

Figure 4: Mean droplet vaporization rate divided by the reference scale defined as $\dot{m}_{d,0} = m_{d,0}/\tau_{d,0}$ with $m_{d,0}$ the initial droplet mass and $\tau_{d,0}$ the initial droplet relaxation time. From left to right: zero, medium, and hight swirl cases.

(red curve in Fig. 5-c) is very similar to the one observed at x/r=30 of the zero-swirl test cases (blue curve in Fig. 5-c). This confirms how the swirl, modifying the jet shape and the mixing layer spread angle, promotes evaporation leading to higher spread of droplet dimensions in regions closer to the inflow.

The joint-PDF of liquid phase volume fraction, Φ, and saturation field sampled by droplets, S, for the axial distance x/r=20, is reported in Fig.6 for the three test cases. For all the swirl numbers, when droplets are not in clusters, corresponding to low volume fraction, we note a clear correlation between the saturation level S with liquid volume fraction Φ, as well as a large variance of the saturation level around its mean conditional values. This means that regions where Φ is low, the dilution is high, and the saturation is low, correspond to the mixing layer regions, where turbulent fluctuations are strong, implying large variance of the saturation level. On the other hand, the regions where the liquid volume fraction is higher correspond to the jet core, and the saturation sampled by droplets is distributed over a narrow range close to fully saturated conditions, i.e $S \simeq 1$. This behaviour appears to be qualitatively similar among the three cases, nonetheless, the swirling effect is to diminish the maximum liquid volume fraction Φ for a given axial distance.

6. Conclusions

The effects of the swirl number on turbulent jet laden with acetone droplets are investigated by means of direct numerical simulation. Regardless of swirl intensity, the evaporation is found to occur in the jet mixing layer, where fresh air entrains the jet, lowers the vapour concentration, and enhances evaporation. This mechanism is found to be responsible of a fast transition from a monodispersed spray to an heterogeneous droplet size distribution. An increase in the swirl intensity is responsible for the increase of the jet spread angle with a consequent diminution of the overall vaporization length. The statistical analysis confirms an enhancement in the evaporation velocity due to the swirling inflow. The mechanisms discussed in the present study are expected to be relevant in all turbulent flows characterized by a mixing layer with entrainment of dry air, such as fuel injectors in combustion chambers. The proper modeling of these mechanisms is pivotal for an improvement of LES and RANS model capabilities, and to accurately reproduce the turbulent vaporization dynamics for both reacting and nonreacting sprays.

DOI: 10.13009/EUCASS2019-891

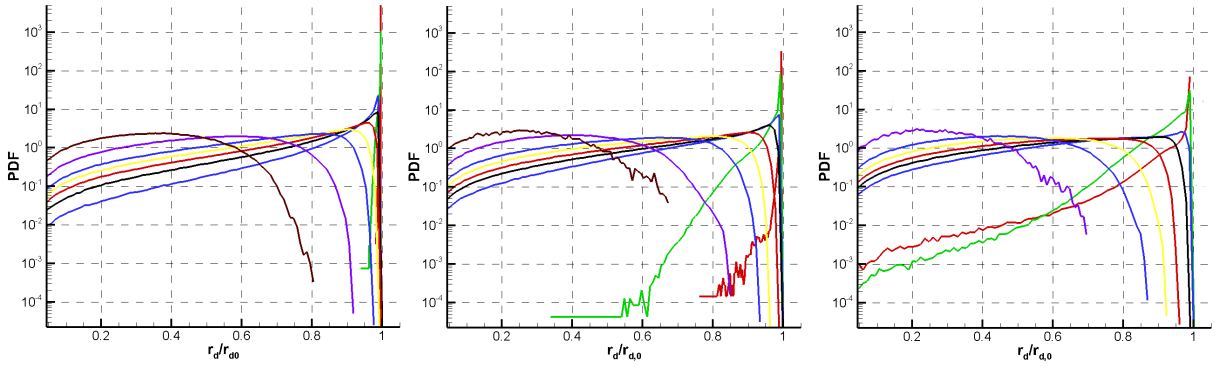

(a) (b) (c)

Figure 5: PDF of droplet non-dimensional radius at various axial distances. From left to right: zero, medium, and high swirl cases.

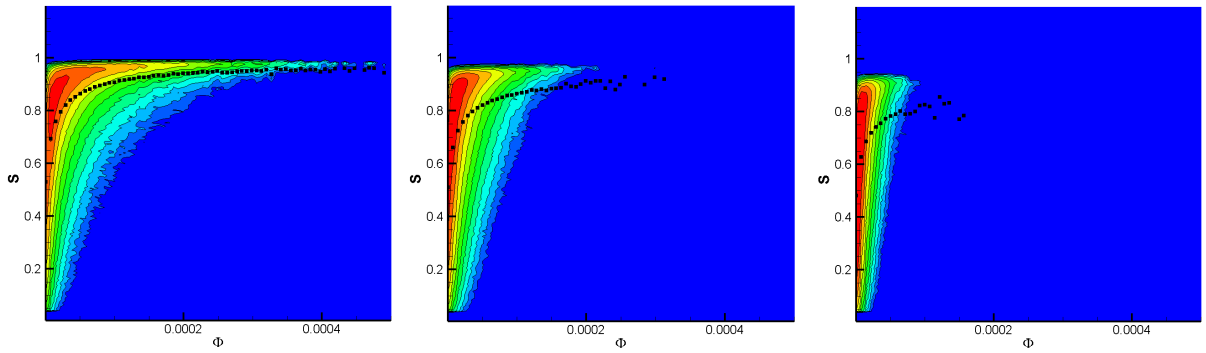

(a) (b) (c)

Figure 6: Joint-PDF of liquid phase volume fraction Φ, and saturation field sampled by droplets, S at axial distance z/D=20. From left to right: zero, medium, and hight swirl cases.

DOI: 10.13009/EUCASS2019-891

7. Acknowledgment

This work is carried out with the support of the Italian Ministry of University and Research (MIUR) and of CCRC/KAUST 1975-03 CCF Subaward Agreement.

References

[1] B. Abramzon and W. A. Sirignano. Droplet vaporization model for spray combustion calculations. *International Journal of Heat and Mass Transfer*, 32(9):1605–1618, 1989.

[2] Federico Dalla Barba and Francesco Picano. Clustering and entrainment effects on the evaporation of dilute droplets in a turbulent jet. *Physical Review Fluids*, 3(3), 2018.

[3] A. Bukhvostova, E. Russo, J. G.M. Kuerten, and Bernard J. Geurts. Comparison of DNS of compressible and incompressible turbulent droplet-laden heated channel flow with phase transition. *ERCOFTAC Series*, 24:181–187, 2018.

[4] Yung Cheng Chen, Sten H. Stårner, and Assaad R. Masri. A detailed experimental investigation of well-defined, turbulent evaporating spray jets of acetone. *International Journal of Multiphase Flow*, 32(4):389–412, 2006.

[5] S. Elghobashi. On Predicting Particle-Laden Turbulent Flows. *Applied Scientific Research*, 52:309–329, 1994.

[6] Koji Fukagata and Nobuhide Kasagi. Highly energy-conservative finite difference method for the cylindrical coordinate system. *Journal of Computational Physics*, 181(2):478–498, 2002.

[7] G. A E Godsave. Studies of the combustion of drops in a fuel spray-the burning of single drops of fuel. *Symposium (International) on Combustion*, 4(1):818–830, 1953.

[8] P. Gualtieri, F. Picano, G. Sardina, and C. M. Casciola. Exact regularized point particle method for multiphase flows in the two-way coupling regime. *Journal of Fluid Mechanics*, 773:520–561, 2015.

[9] Matthew Jemison, Mark Sussman, and Marco Arienti. Compressible, multiphase semi-implicit method with moment of fluid interface representation. *Journal of Computational Physics*, 279:182–217, 2014.

[10] Justin M. Krebs, Adam B. Brame, and Carole C. McIvor. Altered mangrove wetlands as habitat for estuarine nekton: Are dredged channels and tidal creeks equivalent? *Bulletin of Marine Science*, 80(3):839–861, 2007.

[11] A. Lefebvre and V. McDonell. *Atomization and Sprays. Boca Raton: CRC Press,*. Boca Raton: CRC Press, https://doi.org/10.1201/9781315120911, 2017.

[12] Andrew Majda and James Sethian. The derivation and numerical solution of the equations for zero mach number combustion. *Combustion Science and Technology*, 42(3-4):185–205, 1985.

[13] F. Mashayek. Direct numerical simulations of evaporating droplet dispersion in forced low Mach number turbulence. *International Journal of Heat and Mass Transfer*, 41(17):2601–2617, 1998.

[14] R. S. Miller and J. Bellan. Direct numerical simulation of a confined three-dimensional gas mixing layer with one evaporating hydrocarbon-droplet-laden stream. *Journal of Fluid Mechanics*, 384:293–338, 1999.

[15] D B Spalding. THE COMBUSTION OF LIQUID FUELS. *Proc Combust Inst:*, 4:847e64.

[16] E. Villermaux, A. Moutte, M. Amielh, and P. Meunier. Fine structure of the vapor field in evaporating dense sprays. *Physical Review Fluids*, 2(7):1–11, 2017.